Materials Transactions, Vol. 48, No. 8 (2007) pp. 2088 to 2093
Special Issue on Thermoelectric Conversion Materials III

Thermoelectric Properties of Combustion Synthesized and Spark Plasma Sintered $Sr_{1-x}R_xTiO_3$ (R = Y, La, Sm, Gd, Dy, $0 < x \leq 0.1$)

Lihua Zhang[1,*], Tsuyoshi Tosho[2], Noriyuki Okinaka[2] and Tomohiro Akiyama[2]

[1]*Graduate School of Engineering, Hokkaido University, Sapporo 060-8628, Japan*
[2]*Center for Advanced Research of Energy Conversion Materials, Hokkaido University, Sapporo 060-8628, Japan*

Thermoelectric properties of combustion synthesized and spark plasma sintered rare-earth-doped (Y, La, Sm, Gd and Dy) $SrTiO_3$ was investigated from room temperature to 870 K toward the viewpoint of energy and time saving without deterioration in thermoelectric properties. All the rare-earth-doped $SrTiO_3$ were successfully synthesized and sintered with high purities and high densities. With temperature increasing, the absolute value of Seebeck coefficient increased and the electric conductivity decreased; the power factor of all the samples decreased except Y-doped sample in the experimental temperature range. In all the samples, the La-doped $SrTiO_3$ and the Y-doped $SrTiO_3$ had the highest and the lowest power factor, respectively. The dimensionless figure of merit *ZT* of La-doped samples with different doping amount was evaluated and the maximum *ZT* was 0.22, which was obtained at 800 K from $Sr_{0.92}La_{0.08}TiO_3$ sample. Comparing Y and La-doped samples prepared by our method with that of conventional solid-state reaction method, the thermoelectric properties of our samples were relatively higher. Thus the combination of combustion synthesis and spark plasma sintering has a potential to prepare perovskite-oxide materials with relatively higher thermoelectric properties for high-temperature application. [doi:10.2320/matertrans.E-MRA2007836]

(Received November 20, 2006; Accepted March 18, 2007; Published July 25, 2007)

Keywords: *thermoelectric properties, combustion synthesis, spark plasma sintering, rare earth, power factor*

1. Introduction

Thermoelectric material is recently concerned very much because it can be used to convert thermal energy into electric energy directly and vice versa.[1–3] The energy conversion properties of the material is usually evaluated by dimensionless figure of merit *ZT*, which is defined as

$$ZT = T\alpha^2\sigma/\kappa \quad (1)$$

where T, α, σ, and κ are the absolute temperature (K), Seebeck coefficient ($\mu V \cdot K^{-1}$), electric conductivity ($S \cdot m^{-1}$), and thermal conductivity ($W \cdot m^{-1} \cdot K^{-1}$), respectively; $\alpha^2\sigma$ is called power factor ($W \cdot m^{-1} \cdot K^{-2}$).[4,5]

Recently, oxide materials have attracted considerable research interest in thermoelectric application.[6] The layered Co oxide, such as $Na_xCo_2O_4$,[7] shows a low resistivity of 200 $\mu\Omega$ cm accompanied by a large Seebeck coefficient of 100 $\mu V \cdot K^{-1}$. And nonstoichiometric titanium oxide was found to have a *ZT* of 1.64 at 1073 K, which is the largest value for the reported data in this temperature region.[8] As for the *n*-type materials, a typical transition metal perovskite-oxide $SrTiO_3$[9–11] was concerned very much because the electron-doped $SrTiO_3$ has relatively high mobility and large effective mass, which results in high electric conductivity as well as large negative Seebeck coefficient. Okuda *et al.*[12] studied the thermoelectric properties of single crystals $Sr_{1-x}La_xTiO_3$ ($0 \leq x \leq 0.1$) and found a large power factor of 3.6×10^{-3} $Wm^{-1}K^{-2}$ at room temperature, which is comparable to that of practical bismuth telluride alloy. In order to improve the thermoelectric performance, other elements were also partially substituted for Sr or Ti site in the reported study. Muta *et al.*[13] showed an increasing *ZT* value of rare-earth-doped $SrTiO_3$ by decreasing the thermal conductivity without deterioration of the electrical properties. Obara *et al.*[14] measured the thermoelectric properties of Y-doped $SrTiO_3$, and found an increasing in power factor. Ohta *et al.*[15,16] prepared the La- and Nb-doped $SrTiO_3$ single crystals and obtained the maximum *ZT* value of 0.37 (20% Nb doped), which is the largest value among *n*-type perovskite oxide semiconductors ever reported. Although the thermoelectric properties of these electron-doped $SrTiO_3$ were still low compared with the up-to-date intermetallic materials, perovskite oxide has its special advantages, such as good heat resistance and low toxicity; in addition, the material can also have good oxidation resistance at high temperature by using some techniques.[17] Therefore, it has potential for high-temperature *n*-type thermoelectric application.

The polycrystalline perovskite oxide is usually synthesized by the conventional solid-state reaction (SSR) method, which has already been widely used in the production of many electronic ceramics such as PZT (lead-zirconate-titanate ceramics) and $BaTiO_3$.[18–20] However, in SSR method, the materials are usually calcined several times to obtain a homogeneous production; thus this method is time and energy consuming. Therefore, it is necessary to find an economical synthesis method.

Combustion synthesis (CS),[21,22] which uses the energy of an exothermic reaction from the raw materials without any additional energy, has been used to manufacture many inorganic materials such as carbides, nitrides and borides. CS offers many potential advantages over conventional synthesis methods, including relatively simple equipment, shorter processing times, lower energy requirements, higher product purities, and the possibility to synthesize metastable phases. Reportedly, this method has been successfully used to synthesize perovskite oxide with high purity;[23–27] the production of CS is usually porous, which is easy to be ground into fine powder. However, no research has been reported on the thermoelectric properties of CSed perovskite oxides despite their attractiveness from an engineering viewpoint thus far. Therefore, the purpose of this paper is

*Graduate Student, Hokkaido University

to study the possibility of CS to produce perovskite-oxide thermoelectric materials without deterioration in the thermoelectric properties. Based on this consideration, in present study, the CS method was explored for the synthesis of rare-earth-doped $SrTiO_3$ ($Sr_{1-x}R_xTiO_3$, R = Y, La, Sm, Gd and Dy; $0 \leq x \leq 0.1$, simplified as SRTO in this paper) and the synthesized materials were sintered by spark plasma sintering (SPS), which is an efficient method to obtain dense product in a short time. The thermoelectric properties of the product were then compared with those synthesized by the conventional methods.

2. Experimental Procedure

Polycrystalline samples of SRTO were prepared from $SrCO_3$ (99.9% purity, Kanto Chemical, Tokyo, Japan), TiO_2 (99.9% purity, Kojundo Chemical, Sakado, Japan), Ti (99.9% purity, Kojundo Chemical, Sakado, Japan), $NaClO_4$ (98.0% purity, Sigma-Aldrich, St. Louis, USA), and the oxide of doping elements (La_2O_3, Sm_2O_3, Gd_2O_3, Dy_2O_3, 99.9% purity; Y_2O_3, 99.99% purity; Kojundo Chemical, Sakado, Japan). The function and the ratio of TiO_2 to Ti will be discussed later. The desired amounts of the raw materials were mixed by ball milling at 60 rpm for 3 h in air; the raw materials were then placed in a graphite crucible (112 mm × 32 mm × 22 mm) and contacted with a disposable carbon foil that served as the ignitor. The combustion was conducted in argon atmosphere at atmospheric pressure, and the foil was ignited at 50 V and 100 A at room temperature with an internal oxygen supplied from $NaClO_4$. The as synthesized samples were ultrasonic washed to remove solid NaCl and dehydrated in a vacuum drying oven (DP23, Yamato Scientific, Tokyo, Japan), following which, the samples were pulverized into powders by a zirconia mortar and pestle and ground by a planetary ball mill (Pulverisette 6, Fritsch, Idar-Oberstein, Germany) operated at 350 rpm for 40 min in air. The obtained powders were sintered into pellets with a diameter of 10 mm in a graphite die by the SPS (SPS-511S, Sumitomo Coal Mining, Tokyo, Japan). Sintering was carried out for 30 min at a pressure of 34 MPa in vacuum and the sintering temperature was 1573 K.

The phase composition of the samples were analyzed by X-ray diffraction (XRD) (Miniflex, Rigaku, Tokyo, Japan) and scanning electron microscope (SEM) (JSM-7000F, JEOL, Tokyo, Japan). The particle size distribution was measured by the laser scattering particle size distribution analyzer (LA-950, HORIBA, Kyoto, Japan). The electric conductivity and the Seebeck coefficient were simultaneously measured by the Seebeck coefficient/electric resistance measurement system (ZEM-2, ULVAC-RIKO, Yokohama, Japan) from room temperature to 870 K at nitrogen atmosphere. The thermal conductivity was calculated as

$$\kappa = DC_P\rho \tag{2}$$

where D, C_P, and ρ are the thermal diffusivity ($m^2 \cdot s^{-1}$), heat capacity ($J \cdot kg^{-1} \cdot K^{-1}$), and experimental density ($kg \cdot m^{-3}$), respectively. The densities of the samples were measured by the density measurement (Ultrapycnometer 1000, Quantachrome Ltd, Hampshire, Britain), and the thermal diffusivity and the heat capacity were measured by the laser flash thermal constant analyzer (TC-7000, ULVAC-RIKO, Yokohama, Japan).

3. Results and Discussion

The equation of the reaction is as following:

$$(1-x)SrCO_3 + Ti + \frac{x}{2}R_2O_3 + \frac{4-x}{8}NaClO_4 \rightarrow Sr_{1-x}R_xTiO_3 + \frac{4-x}{8}NaCl + (1-x)CO_2 \tag{3}$$

In eq. (3), x is the doping amount; R_2O_3 indicates the rare-earth metal oxide. The adiabatic temperature T_{ad} of eq. (3) was calculated, which is an important parameter in CS. T_{ad} refers to the temperature that would be achieved during the reaction, assuming adiabatic conditions and complete conversion of reactants into final products. For formation of compounds, it has been demonstrated empirically that the reaction will not be self-sustaining unless $T_{ad} \geq 1800$ K.[28] The T_{ad} of eq. (3) was calculated from the general relationship

$$\int_{T_i}^{T_{ad}} \left(\sum_i n_i C_{iP} \right) dT = -\Delta H_r^0 \tag{4}$$

where n_i is the stoichiometric number of the product, C_{iP} is the molar heat capacity of the product, ΔH_r^o is the standard enthalpy of the reaction and T_i is the temperature at which the reaction is triggered. In our experiment, T_i was 298 K. As the result of the calculation, the T_{ad} of eq. (3) was higher than 4000 K, and the reaction was successfully ignited and propagated. However, there still had a little unreacted reagent in the production. It was believed that the high T_{ad} caused a high propagation velocity and then resulted in the incomplete conversion of reactants into final products. Therefore, TiO_2 was added in the raw materials to partly replace Ti. The TiO_2 had a two-fold effect: one was to control the reaction velocity to realize homogeneous production and the other was to decrease the cost of the raw materials. Equation (5) shows the reaction equation.

$$(1-x)SrCO_3 + (1-a)Ti + aTiO_2 + \frac{x}{2}R_2O_3 + \frac{4-4a-x}{8}NaClO_4 \rightarrow Sr_{1-x}R_xTiO_3 + \frac{4-4a-x}{8}NaCl + (1-x)CO_2 \tag{5}$$

In eq. (5), x is the ratio of doping elements, and a is the ratio of TiO_2 amount. According to the research result of Ishikawa *et al.*,[29] when a value is higher than 0.4, the reaction can not be ignited. Therefore, in our study, the TiO_2 ratio a was performed as 0.25 after some exploratory experiments, and the T_{ad} of eq. (5) with $a = 0.25$ was a little higher than 3000 K, which was 1000 K lower than that of the eq. (3). As a result, all the reactions were ignited and propagated fully. After synthesis, the color of the samples changed from gray to dim gray, and there was a layer of white powder on the inside wall of the graphite crucible. From the X-ray diffraction analyses, the white powder was NaCl, which was evaporated during the synthesis. The CSed bulk samples were porous, and the average particle size of the

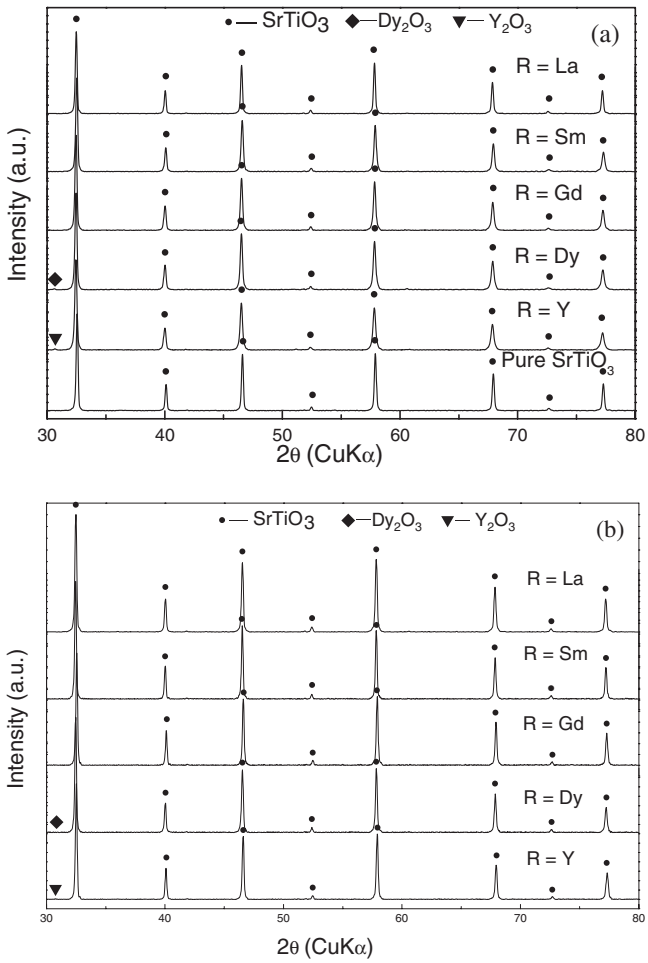

Fig. 1 X-ray diffraction patterns of the CSed SRTO powders (a) before SPS, and (b) after SPS. (The pure $SrTiO_3$ sample was the analytic reagent.)

ground powders before SPS was smaller than 4 μm according to the result of the particle size distribution analyses.

Figure 1(a) and (b) shows the XRD patterns of the CSed SRTO powder before and after sintering, respectively; the XRD pattern of analytic reagent $SrTiO_3$ (99.9% purity, Kojundo Chemical, Sakado, Japan) was also shown in Fig. 1(a). The samples were cubic crystals and no impurity peak was detected in La, Sm, and Gd doped samples. In both (a) and (b), the peaks of Y_2O_3 and Dy_2O_3 were detected in the Y-doped and Dy-doped samples, respectively. However, these impurity peaks were quite small; it indicated that almost all the raw materials were fully reacted during the synthesis by adding appropriated amount of TiO_2. Table 1 shows the lattice parameters of the synthesized samples calculated by XRD data of CSed powder before SPS (standard error $\leq 0.04\%$). In all the samples, Sm, Gd, and Dy-doped samples had a decreased lattice parameter compared with that of $SrTiO_3$, which was similar to the previous report.[13] The decrease of lattice parameter was regarded to be caused by the smaller ionic radius[30] of these rare-earth elements compared with that of Sr^{2+}. The lattice parameter of Y-doped sample is between that of $SrTiO_3$ and Sm, Gd, and Dy-doped samples although the ionic radius of Y is the smallest in all these rare-earth elements; it was considered that the substitution amount of Y for Sr is smaller than 0.05, which caused a relatively higher lattice parameter. The La-doped sample had the same lattice parameter as that of the $SrTiO_3$; it was probably caused by the relatively large ionic radius of La^{3+} compared with other rare-earth elements and the formation of Ti^{3+}, the ionic radius of which was larger that that of Ti^{4+}.[13]

Table 1 Characteristics of rare-earth-doped $SrTiO_3$.

Sample	Lattice constant, a/nm (Before SPS)	Bulk density (After SPS)	
		ρ/kg·m^{-3}	%T.D.
$SrTiO_3$	0.3905	—	—
$Sr_{0.95}La_{0.05}TiO_3$	0.3905	4.95×10^3	95.6
$Sr_{0.95}Sm_{0.05}TiO_3$	0.3903	5.11×10^3	98.0
$Sr_{0.95}Gd_{0.05}TiO_3$	0.3903	4.97×10^3	95.1
$Sr_{0.95}Dy_{0.05}TiO_3$	0.3903	5.23×10^3	99.9
$Sr_{0.95}Y_{0.05}TiO_3$	0.3904	5.02×10^3	98.0

Figure 2 shows the SEM cross-section images of the as synthesized SRTO bulk. The samples had homogeneous microstructures with few voids and small grains. The grain growth in $SrTiO_3$ has been reported to be highly sensitive to donor doping. At low donor concentrations, grain growth may become pronounced during high temperature sintering, often resulting in 50–100 μm.[31–33] The grain size of our samples varies in the range 2–10 μm, which was relatively small. As shown in Table 1, the bulk densities of these samples were higher than 95% of the theoretical densities, which were much higher than the reported data[13,34] of rare-earth doped $SrTiO_3$ prepared by SSR. The high density of our samples was considered to be caused by the smaller particle size and higher surface areas of our CSed powder compared with those prepared by SSR, which helped the acceleration of sintering at relatively lower temperature, and the grain size increase could also be controlled by SPS sintering method. Thus, the high purity rare-earth-doped $SrTiO_3$ with high density was successfully obtained by CS and SPS.

Figure 3 and Figure 4 show the temperature and the doping element dependence on the Seebeck coefficient and electric conductivity, respectively. The Seebeck coefficient of all the samples was negative in the temperature range considered, which indicated that the samples were *n* type. With the temperature increasing, the absolute value of Seebeck coefficient increased and electric conductivity decreased, showing the metallic behavior. And the electric conductivity of the La, Sm, Gd, and Dy doped samples was relatively higher compared with the reported data[13] of SSR method. Furthermore, the absolute value of the Seebeck coefficient and electric conductivity had a reverse sequence with different doping element. In all the samples, the Y-doped sample had much different value from the other elements doped samples in Seebeck coefficient and electric conductivity, in which the Seebeck coefficient was the highest and the electric conductivity was the lowest. On the other hand, the other elements doped samples had a close Seebeck coefficient and electric conductivity. The difference in Seebeck coefficient and electric conductivity indicated that the carrier density of Y-doped sample was smaller than the other samples; the Y substitution amount was considered to be lower than our expected doping amount 0.05, which also caused the relatively higher lattice constant. In Fig. 3, the

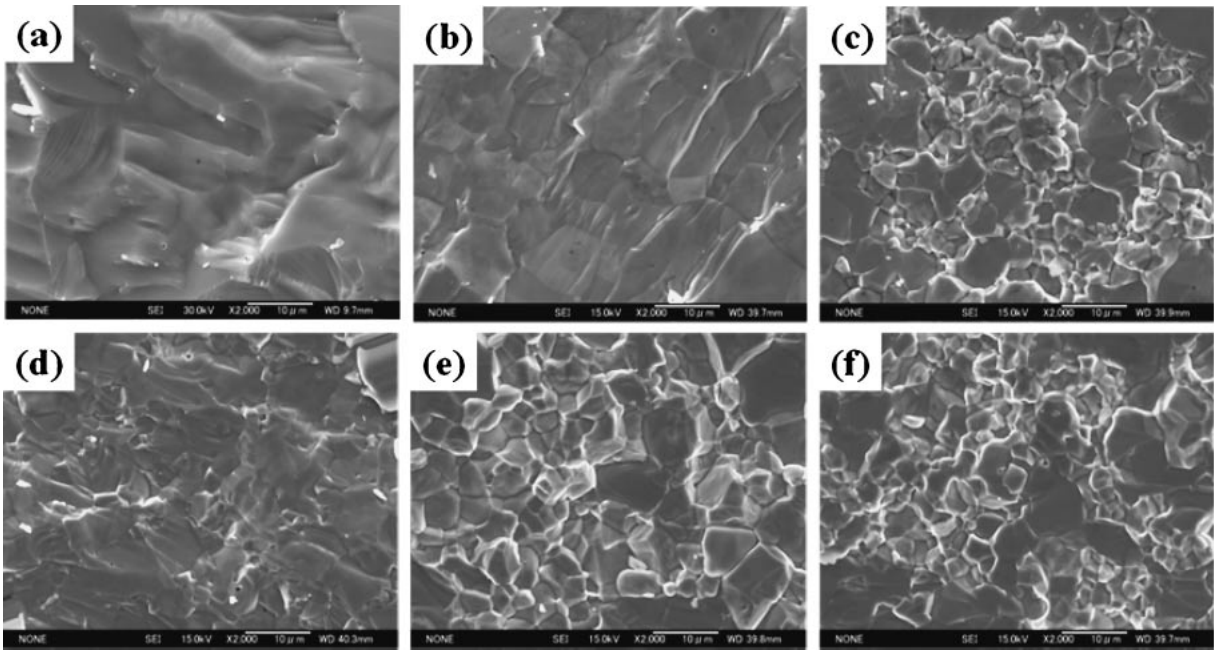

Fig. 2 Scanning electron microscopy cross-section images of sintered $SrTiO_3$ and $Sr_{0.95}R_{0.05}TiO_3$, (a) $SrTiO_3$, (b) R = Y, (c) R = La, (d) R = Sm, (e) R = Gd, and (f) R = Dy.

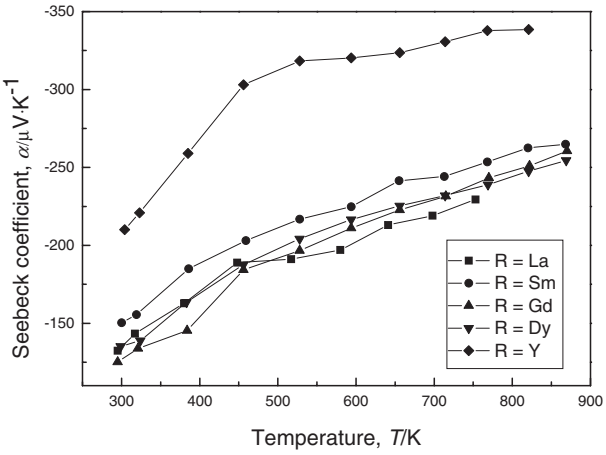

Fig. 3 Temperature dependence on the Seebeck coefficient of SRTO.

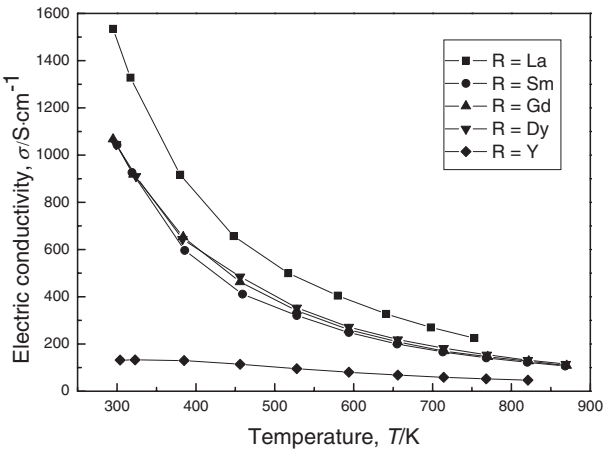

Fig. 4 Temperature dependence on the electric conductivity of SRTO.

increasing slope of Seebeck coefficient for Y-doped sample had an obviously change at 528 K. The reason of this phenomenon was not very clear at present time; and it was probably caused by the change of dominant mechanism of carrier scattering.

Figure 5 shows the temperature and the doping element dependence on the power factor, which was calculated by Seebeck coefficient and electric conductivity. With temperature increasing, the power factor of La, Dy, Gd, and Sm-doped samples decreased; the power factor of Y-doped sample increased firstly then decreased and the highest power factor was $1.04 \times 10^{-3}\,W{\cdot}m^{-1}{\cdot}K^{-1}$ obtained at 456 K. Comparing our Y-doped sample with the reported data[14] synthesized by SSR and sintered by hot pressing technique at 1673 K for 1 h under a pressure of 100 MPa, the temperature dependencies on the power factor were similar to the reported data, and our sample had a relatively higher power factor and

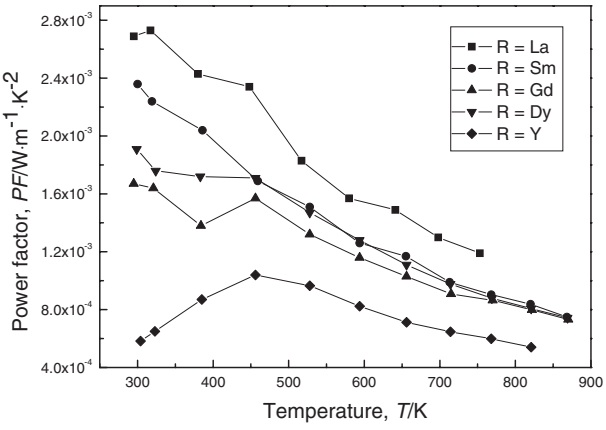

Fig. 5 Temperature dependence on the power factor of SRTO.

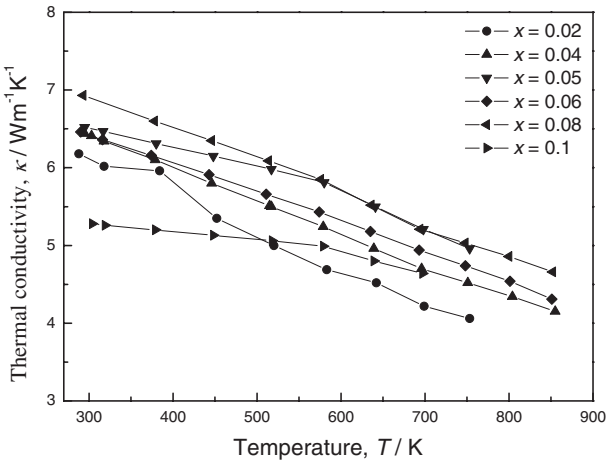

Fig. 6 Temperature and La doping amount dependence on thermal conductivity of $Sr_{1-x}La_xTiO_3$.

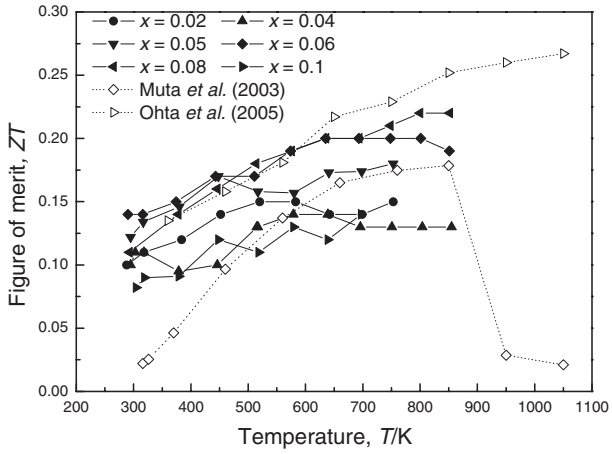

Fig. 7 Temperature and La doping amount dependence on *ZT* value of $Sr_{1-x}La_xTiO_3$, together with recently reported data.[13,15]

the maximum power factor of our Y-doped sample was more than one time higher than the reference data. It was considered that the high density of our sample caused the higher electric conductivity, which resulted in the higher power factor. In all these rare-earth-doped $SrTiO_3$, the La-doped sample had the highest power factor and Y-doped sample had the lowest power factor. The Dy, Gd and Sm doped samples had a similar power factor in the temperature range from 440 K to 870 K, which was caused by the similar Seebeck coefficient and electric conductivity as shown in Fig. 3 and Fig. 4.

The thermal conductivity of the La-doped samples $Sr_{1-x}La_xTiO_3$ ($0 < x \leq 0.1$) with different doping amount was evaluated and showed in Fig. 6. With temperature increasing, the thermal conductivity decreased, caused by the decrease in the thermal diffusivity. All the thermal conductivity was lower than the reported single crystal samples[15] because of the phonon scattering of the grain boundary in polycrystal. Compared them with the reported polycrystal sample,[13] although the density of our samples was much higher than the reported data, the thermal conductivity was only a little higher, which indicated the relatively small grain size of our samples compensated the large difference in the density between our samples and the reported ones. Figure 7 shows the temperature and doping amount dependences on *ZT* value of La doped $SrTiO_3$. We compared our samples with the reference data[13,15] of single crystal samples and polycrystals prepared by SSR, in which the single crystal samples was the highest *ZT* record of La-doped $SrTiO_3$. In the temperature range considered, overall, *ZT* increased with temperature; it had a tendency to increase at even higher temperatures; this showed that the material was suitable for high-temperature application. Among all the La-doped $SrTiO_3$, the $Sr_{0.92}La_{0.08}TiO_3$ sample showed the largest *ZT* 0.22 at 800 K; this value was close to the highest record of the La-doped $SrTiO_3$[15] at the same temperature. Furthermore, the *ZT* values of our samples were comparable to the reported data[13] prepared by SSR method, and some were even higher than the reported data because of the relatively higher electric conductivity of our samples. It indicated that the CS combined with SPS is an appropriate method to prepare the perovskite oxide materials for thermoelectric application because the production has high density and small grain size, which can increase the electric conductivity and decrease the thermal conductivity.

As for the other rare-earth-doped $SrTiO_3$, according to the reported thermal conductivity data,[13] the *ZT* value was estimated between 0.15 and 0.3, which was relatively higher for the electric-doped $SrTiO_3$. Thus, our samples had the potential in relatively higher *ZT* value compared with the reported data. These results showed that CS is an effective method to synthesis perovskite oxide materials and the high-density samples can be successfully obtained by SPS, in which the electric conductivity of the samples is improved. The thermoelectric properties of the production was comparable to that prepared by conventional methods. Thus, it is possible to get an improvement in thermoelectric properties by using CS combined with SPS technique to synthesize perovskite-oxide thermoelectric materials for high-temperature application.

4. Conclusion

Combustion synthesis, combined with spark plasma sintering, was used to produce rare-earth-doped $SrTiO_3$ perovskite-oxide materials for high-temperature thermoelectric application. The following results were obtained:

(1) The desired high purity products with various doping elements were successfully combustion synthesized and sintered with high density by spark plasma sintering.
(2) In the temperature range considered, all the SRTO were *n*-type materials, and the Y-doped sample had the highest absolute value of Seebeck coefficient and the lowest electric conductivity among all the doping rare-earth elements.
(3) With temperature increasing, the power factor of Y-doped sample increased firstly and then decreased. In contrast, the other elements doped samples had a decreasing power factor with temperature on the whole.
(4) In all the rare-earth-doped $SrTiO_3$ samples, the highest and lowest power factor was obtained in the La-doped sample and Y-doped sample, respectively.

(5) With temperature increasing, the *ZT* of the La-doped $SrTiO_3$ with various doping amount from 0.02 to 0.1 showed an increasing tendency, and the maximum *ZT* of 0.22 was obtained with a doping amount of 0.08 at 800 K.
(6) The high density of our samples improved the electric conductivity; compared with the reference data, the thermoelectric properties of our Y and La-doped samples were relatively higher than the conventional SSR method.

All the results proved that combustion synthesis combined with spark plasma sintering was a promising method to produce perovskite-oxide thermoelectric materials without deterioration of the thermoelectric properties.

Acknowledgement

The authors acknowledge 21st Century COE Program "Topological Science and Technology" for the financially supported in part and Mr. Kenji Ohkubo for his assistance in the thermal conductivity measurement.

REFERENCES

1) T. J. Seebeck: Abhandlungen der Deutschen Akademie der Wissenschaften zu Berlin. **265** (1823) 1822–1823.
2) J. C. Peltier: Ann. Chim. **LV1** (1834) 371.
3) B. Raton: *CRC Handbook of Thermoelectrics*, (CRC, Florida, 1995) pp. 1–5.
4) E. Altenkirch: Phys. Z. **10** (1909) 560.
5) E. Altenkirch: Phys. Z. **12** (1949) 920.
6) K. Koumoto, I. Terasaki and R. Funahashi: MRS Bull. **31** (2006) 206–210.
7) I. Terasaki, Y. Sasago and K. Uchinokura: Phys. Rev. B: Condens. Matter. **56** (1997) 12685–12687.
8) N. Okinaka and T. Akiyama: Jpn. J. Appl. Phys. **45** (2006) 7009–7010.
9) H. Muta, K. Kurosaki and S. Yamanaka: J. Alloys. Compd. **368** (2004) 22–24.
10) T. Maekawa, K. Kurosaki, H. Muta, M. Uno and S. Yamanaka: J. Alloys. Compd. **387** (2005) 56–59.
11) H. Muta, K. Kurosaki and K. Yamanaka: J. Alloys Compd. **392** (2005) 306–309.
12) T. Okuda, K. Nakanishi, S. Miyasaka and Y. Tokura: Phys. Rev. B: Condens. Matter. **63** (2001) 113104.
13) H. Muta, K. Kurosaki and S. Yamanaka: J. Alloys Compd. **350** (2003) 292–295.
14) H. Obara, A. Yamamoto, C. H. Lee, K. Kobayashi, A. Matsumoto and R. Funahashi: Jpn. J. Appl. Phys. **43** (2004) 540–542.
15) S. Ohta, T. Nomura, H. Ohta and K. Koumoto: J. Appl. Phys. **97** (2005) 034106.
16) S. Ohta, T. Nomura, H. Ohta, M. Hirana, H. Hosono and K. Koumoto: Appl. Phys. Lett. **87** (2005) 092108.
17) A. Grill, C. Jahnes and C. Jr. Cabral: J. Mater. Res. **14** (1999) 1604–1609.
18) H. Oguchi, C. Ando, H. Chazono, H. Kishi and M. Senna: J. Phys. IV France **128** (2005) 33–39.
19) Y. Hayashi, T. Kimura and T. Yamaguchi: J. Maters. Sci. **21** (1986) 757–762.
20) R. N. Viswanath, H. Thangasamy, S. Ramasamy and N. Karuppiah: Bull. Electrochem. **9** (1993) 293.
21) J. Poth, R. Haberkorn and H. P. Beck: J. Eur. Ceram. Soc. **20** (2000) 707–713.
22) J. Poth, R. Haberkorn and H. P. Beck: J. Eur. Ceram. Soc. **20** (2000) 715–723.
23) A. G. Merzhanov: Ceram. Int. **21** (1995) 371–379.
24) T. Akiyama, H. Isogai and J. Yagi: AIChE J. **44** (1998) 695–700.
25) Q. Ming, M. D. Nersesyan, J. T. Richardson, D. Luss and A. A. Shiryaev: J. Maters. Sci. **35** (2000) 3599–3606.
26) A. V. Komarov, I. P. Parkin and M. Odlyha: J. Maters. Sci. **31** (1996) 5033–5037.
27) H. Ishikawa, M. Enoki, T. Ishihara and T. Akiyama: Int. J. SHS **15** (2006) 259–267.
28) A. Varma and J. P. Lebrat: Chem. Eng. Sci. **47** (1992) 2179–2194.
29) H. Ishikawa, K. Oohira, T. Nakajima and T. Akiyama: J. Alloy. Compd. Submitted.
30) R. D. Shannon: Acta Cryst. A **32** (1976) 751–767.
31) I. Burn and S. Neirman: J. Mater. Sci. **17** (1982) 3510–3524.
32) M. F. Yan: Mater. Sci. Eng. **48** (1981) 53–72.
33) M. Kahn: J. Am. Ceram. Soc. **54** (1971) 452–457.
34) S. Hui and A. Petric: J. Electrochem. Soc. **149** (2002) J1–J10.